CONFIDENTIAL

Copy
RM E55A26

NACA RM E55A26

NACA

RESEARCH MEMORANDUM

STABILIZATION TECHNIQUES FOR RAMP-TYPE SIDE INLETS AT SUPERSONIC SPEEDS

By L. J. Obery, R. W. Cubbison, and T. G. Mercer

Lewis Flight Propulsion Laboratory
Cleveland, Ohio

NATIONAL ADVISORY COMMITTEE
FOR AERONAUTICS

WASHINGTON

April 11, 1955

CONFIDENTIAL

NATIONAL ADVISORY COMMITTEE FOR AERONAUTICS

RESEARCH MEMORANDUM

STABILIZATION TECHNIQUES FOR RAMP-TYPE SIDE INLETS AT SUPERSONIC SPEEDS

By L. J. Obery, R. W. Cubbison, and T. G. Mercer

SUMMARY

Methods of increasing the stable subcritical range of a twin-duct double-ramp inlet mounted on the sides of a fuselage forebody were investigated in the Lewis 8- by 6-foot supersonic wind tunnel. For operation at a free-stream Mach number of 2.0 with the twin ducts separated by an internal splitter plate, increasing the length of zero diffusion in the initial part of the subsonic diffuser from 1 to 3 hydraulic diameters increased the stable subcritical range from about 10 percent of critical mass-flow ratio with the shortest to about 15 percent with the longest length of zero diffusion. For combined duct operation (no splitter plate), bleeding the boundary layer from the ramp increased the inlet stable range from 12 percent of critical flow with the no-bleed inlet to 24 percent with the ramp-bleed inlet. Removal of the ramp boundary layer by a flush slot near the inlet throat increased the stable range to about 18 percent of critical flow, but also increased the diffuser total-pressure recovery by more than $2\frac{1}{2}$ percent. Removal of the inlet side fairings resulted in a decrease in total-pressure recovery and maximum capture mass-flow ratio without an appreciable increase in the stable range.

At approximately engine-idle mass-flow requirements at a free-stream Mach number of 2.0, stable inlet operation could be obtained by increasing the second-ramp angle to 30°. Stable regulation to low mass-flow ratios at Mach number 2.0 was not possible with a second-ramp angle of 0°.

INTRODUCTION

Stable mass-flow regulation of an air-induction system for turbojet-powered aircraft must be provided for at least two flight conditions. First, during maneuvering the inlet may experience a reduction in mass flow of as much as 10 to 15 percent of design air flow. Satisfactory operation from consideration of the engine, the aircraft structure, and

the pilot necessitates that the reduced mass flow be obtained without flow pulsation. Furthermore, this condition must be satisfied without either excessive loss in pressure recovery or an appreciable increase in inlet drag. Secondly, throttle closure to idle setting at high flight speed, as could occur, for example, in a dive or an emergency, would restrict the inlet mass-flow ratio to much lower values. It is necessary that the inlet system remain pulse-free during the time required to decelerate the airplane to low supersonic speeds. Because aircraft deceleration is the desired objective, the satisfaction of this condition imposes no requirement on the loss of pressure recovery or the increase in inlet drag.

Methods of increasing the stable subcritical range of annular nose inlets (nacelle-type installations) have been demonstrated experimentally. One technique is the addition of lengths of nearly constant-area sections to the initial portion of the subsonic diffuser as reported, for example, in references 1 and 2. Another method involves the removal of the separated or thickened boundary layer resulting from interaction between the inlet terminal shock and the compression-surface boundary layer. References 3 to 5, for example, indicate that boundary-layer removal at or immediately aft of the compression surface increased the inlet stable subcritical range.

The purposes of this investigation were (1) to determine whether the stable subcritical range of a twin-duct air-intake system with two-dimensional ramp inlets could be increased by using the same techniques already demonstrated on annular nose inlets without prohibitively decreasing the inlet performance and (2) to provide stable operation at very low mass-flow ratios without regard to inlet performance. The investigation was conducted in the Lewis 8- by 6-foot supersonic wind tunnel over a range of mass-flow ratios and at Mach numbers of 1.5, 1.8, and 2.0.

SYMBOLS

The following symbols are used in this report:

A	area
D_h	hydraulic diameter, $\frac{4 \times \text{inlet area}}{\text{wetted perimeter}}$, 3.41 in.
L	length of subsonic diffuser, 81.5 in.
M	Mach number
m_3/m_0	mass-flow ratio, $\frac{\text{mass flow}}{\rho_0 V_0 A_i}$

$(m_3/m_0)_{max}$	maximum capture mass-flow ratio of any inlet
$(m_3/m_0)_{min}$	minimum value of stable mass-flow ratio of any inlet
P	total pressure
$\Delta P_f/P_0$	ratio of half-amplitude total-pressure fluctuation to free-stream total pressure
p	static pressure
V	velocity
x	distance from cowl lip, model station 36
λ	angle of second ramp with respect to free-stream direction
ρ	mass density of air

Subscripts:

x	conditions at x-distance from cowl lip
0	free stream
3	diffuser-exit survey station, model station 100

Pertinent areas:

A_i	projected frontal area of both inlets, 0.3646 sq ft
A_3	flow area at diffuser discharge, 0.457 sq ft

APPARATUS AND PROCEDURE

The model of the present investigation is illustrated photographically in figure 1 and schematically in figure 2. Shown in these figures are the twin double-ramp side inlets mounted on the 1/4-scale fuselage forebody of a supersonic airplane. The ducts were geometrically similar and joined into a common duct at a model station corresponding to the compressor face.

Details of the model, including internal flow stations and representative model cross sections, are shown in figure 2. The nose of the model was canted down at an angle of 5°, and the inlets were canted down at an

angle of 3° with respect to the fuselage centerline. The 5° droop of the nose was intended to improve pilot vision in the prototype rather than to influence flow conditions for maximum performance.

Photographs and schematic drawings of the inlets are shown in figure 3. The inlet had a 9° first-compression ramp and an 18° second-compression ramp; the second ramp was also varied to 0° and 30°. The leading edge of the first ramp was positioned so that the resulting oblique shock was located just ahead of the cowl lip at Mach number 2.0. The first ramp also acted as a boundary-layer splitter plate and completely removed the fuselage boundary layer.

Figure 3(a) shows profiles of the three stabilizing sections designed to provide lengths of approximately 1, 2.3, or 3 hydraulic diameters of nearly constant flow area in the initial portion of the subsonic diffuser. A slight area expansion was allowed in the longest section for boundary-layer growth. During the investigation of the three stabilizing sections, the ducts were separated by a splitter plate, which extended from station 98.75 (fig. 2) past the choking exit. The splitter plate was then removed to allow the twin ducts to operate as a unit. The details of the ramp boundary-layer-removal apparatus are shown in figures 3(b), (c), and (e). Boundary-layer air was bled from the inlet into the fuselage and discharged to the free stream. As with the inlets of reference 6, no attempt was made to measure or meter the bleed air other than that resulting from choking at the slot or the perforations. The 3-hydraulic-diameter stabilizing section was used with the flush-slot and perforated-ramp inlets.

One of the configurations investigated had the side fairings removed (fig. 3(d)). This inlet also had a 3-hydraulic-diameter stabilizing section. Figures 3(f) and (g) show details of the 0° and 30° second-ramp inlets. The internal contour shown in figure 3(f) simulates the subsonic diffuser section aft of the second ramp when the angle of the second ramp has been reduced to 0°. Although the second ramp in the prototype is mechanically variable, all configuration changes were made on the model by removing and replacing appropriate contoured blocks. The effect of the various configurations on the area variation of the subsonic diffuser is shown in figure 4.

The pressure fluctuations in the ducts were measured with a pitot tube located approximately 1/2 inch from the duct wall. The tube was placed just aft of that part of the duct common to all configurations or about 30 inches from the first-ramp leading edge.

The model instrumentation was the same as that of reference 7 except that total-pressure rakes in the inlet ducting at station 40 and the boundary-layer total-pressure rakes were not used. No force measurements were made during this investigation. Except for the fuselage boundary-layer mass flow, the computational methods were also the same as those described in reference 7.

The investigation was conducted at free-stream Mach numbers of 2.0, 1.8, and 1.5, at a fuselage angle of attack of $3\frac{1}{2}^{\circ}$ corresponding to an inlet angle of attack of about 0°, and for a range of mass-flow ratios. The Mach number immediately ahead of the inlet, outside the boundary layer, was essentially constant across the inlet face at about the free-stream value. The Reynolds number of the tunnel was approximately 4.3×10^6 per foot of length.

RESULTS AND DISCUSSION

The results of the present investigation will be discussed in two parts: (1) Stabilization of a high-performance inlet at relatively high mass-flow ratios will be considered. In this range, the methods of inlet stabilization should not unduly penalize the inlet performance either in total-pressure recovery or by increased inlet drag. (2) Methods of stable inlet operation at engine-idle air-flow requirements as would occur from throttle closure at supersonic speeds will be discussed. For this operation, high inlet drag and/or low total-pressure recovery may actually be desirable since rapid airplane deceleration is required.

Stabilization with High Performance

It has been demonstrated (refs. 1 and 2) that inlet stabilization may be accomplished by providing some length of constant-area section in the initial part of the subsonic diffuser. The internal performance and stability characteristics at $M_0 = 2.0$ of the left ducts of three configurations with splitter plate are presented in figure 5. The results of the left ducts are presented because different performances between the right and left ducts were noted for the inlet with 3-hydraulic-diameter stabilizing sections, probably as a result of slight dimensional differences. As the length of constant-area section was increased from 1 to 3 hydraulic diameters, an increase in stability of the order of 5 percent of critical mass-flow ratio was realized (fig. 5(b)). The increase was accompanied by small changes in critical and peak total-pressure recovery (fig. 5(a)).

As shown in figure 6, removal of the splitter plate from the 3-hydraulic-diameter stabilizing-section configuration reduced the stable range from the single-duct value of about 15 percent of critical mass-flow ratio to about 12 percent for the combined-duct system. Although data are not presented, the right-duct performance for the configuration with splitter plate was nearly identical to the twin-duct performance. Because of the different flows in the two ducts, the twin-duct system was only as stable as the least stable duct. Removing the splitter plate, however, had no appreciable effect on the critical and peak total-pressure recoveries.

The effect on inlet stable mass-flow range of removing the boundary layer at or immediately aft of the second compression surface was investigated in conjunction with the 3-hydraulic-diameter zero-diffusion section. As shown in figure 7, bleeding the boundary layer from the ramp increased the stable regulation range from about 12 percent with the no-bleed inlet to about 24 percent with the perforated-ramp inlet, with no change in critical total-pressure recovery and a reduction of only 1 percent of the inlet maximum capture mass flow. Removal of the boundary layer by means of a flush slot located near the inlet throat increased the inlet stable subcritical range from 12 percent of critical flow with the no-bleed inlet to 18 percent for the flush-slot inlet. The mass-flow ratio was reduced about 4 percent, but the diffuser critical total-pressure recovery was increased by $2\frac{1}{2}$ percent. The higher recovery may have resulted from shock - boundary-layer interaction in the manner described in reference 8. Presumably, the terminal shock separated the ramp boundary layer, thus effectively forming an added compression wedge and increasing the total-pressure recovery through the lambda portion of the inlet shock system. Removal of the separated flow was then effected by the flush slot before it could adversely affect the subsonic diffusion.

The boundary layer along the side fairings is subjected to the same high-pressure gradient and interaction from the inlet terminal shock as the ramp boundary layer. Therefore, it was surmised that the removal of the side fairings, thereby removing a source of boundary-layer interaction, would increase the inlet stability range. However, as shown in figure 8, removal of the side fairings did not increase the stable operating range appreciably. The critical total-pressure recovery and maximum capture mass-flow ratio were reduced, both on the order of 6 percent, as a result of flow spillage around the ramp sides with the attendant reduction in supersonic compression. The maximum variation in total-pressure recovery across the diffuser exit face, with or without side fairings, was approximately 8 percent at critical inlet flow.

Figure 9 presents schlieren photographs of the perforated-ramp inlet, showing its operation progressively from the supercritical range (fig. 9(a)) through the subcritical range (figs. 9(b) and (c)) and into the low-mass-flow region (fig. 9(d)). At the minimum stable point (fig. 9(c)), different mass flows occurred in the two ducts, as indicated by the different displacements of the inlet terminal shocks from the cowl lips. In the low-mass-flow range, one duct operated supercritically, and reverse flow occurred in the other. As shown in figure 9(d), the terminal shock from the reverse-flow duct separated the fuselage boundary layer and formed an oblique shock far ahead of the inlet. No tendency was noted for the oblique shock from the fuselage to oscillate from one duct to the other. The external shock pattern for the supercritical inlet under these conditions was stationary.

Pulsing is arbitrarily defined herein as any total-pressure variation of half-amplitude greater than $2\frac{1}{2}$ percent of free-stream total pressure. The half-amplitudes of the peak fluctuations occurring in either duct are presented in figure 10. The fairing of the curves in this figure was not arbitrary but was guided by pressure traces taken during slow transient operation of the mass-flow control plug. For the configurations with splitter plate, the amplitude of pressure fluctuations steadily increased after pulsing began. At a given mass-flow ratio in the pulsing region, the amplitude of the pressure fluctuation increased as the length of constant-area stabilizing section was increased from 1 to 3 hydraulic diameters. For combined duct operation, at some low value of mass-flow ratio one of the ducts operated supercritically and the other carried little flow (as shown in the schlieren picture of fig. 9(d)). For the perforated-ramp inlet at that condition ($m_3/m_0 < 0.44$), the maximum half-amplitude suddenly increased to about three times the magnitude of the pulse that occurred when the ducts operated at nearly equal air flows. For the no-side-fairing inlet, however, operation at mass flows below 0.42 (one duct supercritical, reverse flow in other) was accompanied by a sudden decrease in the peak magnitude of fluctuation. Peak half-amplitudes for the no-side-fairing inlet reached values greater than 30 percent of free-stream total pressure.

In the stable subcritical region of the configurations with splitter plate, pressure fluctuations of small amplitude were noted. During pulsing operation (point A in fig. 10), the pulse in both ducts was quite regular, as shown in figure 11(a). The separated ducts pulsed with a frequency of about 30 cycles per second regardless of stabilizing section length. Removal of the splitter plate caused the system to pulse in a much more complicated, and at times almost random, manner. Regardless of the particular inlet configuration, operation in the low-mass-flow region resulted in one duct operating supercritically and little or no flow in the other (as discussed previously and shown in fig. 9(d)). This type of operation was characterized by a high-amplitude, low-frequency pulse in the supercritical duct and very-low-amplitude fluctuation in the reverse-flow duct, as illustrated by figure 11(b) corresponding to point B in figure 10. From control-room observations and high-speed schlieren photography, it was noted that the oblique-shock configuration of the supercritical inlet did not fluctuate. The movement of the inlet terminal shock therefore was confined to inside the duct. The no-side-fairing inlet at peak amplitude (fig. 10, point C) with approximately equal flow in both ducts showed high-amplitude, low-frequency pulsations combined with fluctuations of considerably less amplitude but higher frequency as shown in figure 11(c).

Low-Mass-Flow Stabilization

For operation at inlet mass flows corresponding to engine-idle requirements, the air-inlet system must remain pulse-free during the time necessary to decelerate to low supersonic speeds. To obtain the required stability in the low-mass-flow range, two methods were investigated: First, since normal-shock inlets are usually stable to the low-mass-flow range (ref. 9), the second-ramp angle was reduced to 0°. The inlet deviated from the conventional normal-shock inlet in that the 0° ramp was preceded by an expansion region following the 9° first compression ramp. The second method was to restrict the inlet throat area to allow only a specified amount of flow to enter the inlet. For this particular investigation, the desired throat area was obtained by increasing the second-ramp angle to 30°.

In the following discussion it is assumed for illustrative purposes that engine-idle air-flow requirements correspond approximately to inlet mass-flow ratios of 40 percent. During the reduction of the mass-flow ratio to 40 percent at $M_0 = 2.0$ (fig. 12(a)), the air-intake system would have been subjected to pulsing with the 18° and the 0° second-ramp inlets. The 30° second-ramp inlet lowered the critical mass flow to approximately 0.58, and the stable range of the inlet would allow pulse-free operation at engine-idle conditions. Had this stable range not been available, the angle of the second ramp could have been increased to reduce the critical mass-flow ratio still further. The minimum mass-flow-ratio data points presented for the 30° second-ramp inlet at all Mach numbers were determined by the limit of mass-flow control plug travel and do not represent the limit of stable regulation. The 30° second ramp detached the shock wave from the leading edge of the second ramp and reduced the critical total-pressure recovery to about 79 percent from the 86 percent obtained with the 3-hydraulic-diameter, 18° second-ramp inlet. The inlet drag probably also increased; however, because the immediate purpose for throttle closure is airplane deceleration, high inlet drag and/or low total-pressure recovery may actually be desirable.

At a free-stream Mach number of 1.8 (fig. 12(b)), the stable range of the 18° second-ramp inlet was still insufficient to allow pulse-free operation at 40 percent mass-flow ratio. However, the much greater stable range at $M_0 = 1.8$ over that at $M_0 = 2.0$ indicates that a ramp angle between 18° and 30° would have given the required stable operation. At $M_0 = 1.5$, the 18° second-ramp inlet allowed pulse-free operation to 40 percent mass-flow ratio; however, the range of stable regulation lower than 40 percent was quite limited.

Reduction of the mass-flow ratio following throttle closure at a free-stream Mach number of 2.0 with the basic 18° second ramp would have subjected the inlet system to pressure fluctuations of as much as 11

percent of the free-stream total pressure (fig. 13(a)). From design considerations, pressure fluctuations of this order may be detrimental to the structure. When the second-ramp angle was reduced to 0° no fluctuation-free flow could be obtained either in the supercritical or subcritical region, although, as shown in figure 13(a), the amplitude during part of the subcritical range was smaller than that defined as pulsing. In the pulsing region, the amplitude of the fluctuations first increased to a peak of approximately 6 percent of the free-stream total pressure and then decreased almost to the stable-pulsing boundary. The pressure fluctuations noted for the 30° second-ramp inlet never reached the region defined as pulsing, although half-amplitudes as high as 2 percent of free-stream total pressure were recorded.

The total-pressure distributions at the compressor face reveal an additional problem for operation at low mass flows where the flow may be forced through one duct only. As a typical example for the 0° second-ramp inlet during this type of operation (fig. 14(a)), there would be a total-pressure variation of 35 percent across the compressor face, which may be untenable from duct or compressor structural considerations. The 30° second-ramp inlet is also subject to the same type distribution; however, the total-pressure difference is considerably smaller, on the order of 5 percent (fig. 14(b)).

Schlieren photographs of the 30° second-ramp inlets are shown in figure 15. A definite separation of the boundary layer ahead of the intersection of the first and second ramp of the 30° second-ramp inlet can be seen in figures 15(a) and (b). There is an absence of a clearly defined normal shock in the subcritical range (figs. 15(b) and (c)). The tendency of one duct to capture less mass flow than the other as operation progressed into the subcritical range (resulting in the pressure distribution of fig. 14(b)) is evident in figures 15(b) and (c).

SUMMARY OF RESULTS

An investigation was conducted in the Lewis 8- by 6-foot supersonic wind tunnel to explore methods of increasing the stable subcritical mass-flow range of a twin-duct double-ramp inlet mounted on the sides of a fuselage forebody at Mach numbers from 1.5 to 2.0. Stable operation was required for two phases of inlet operation: (1) Limited stable subcritical range near critical inlet mass-flow ratio was required without excessively penalizing the inlet performance, and (2) pulse-free operation to very low mass-flow ratios corresponding to engine-idle air-flow requirements was desired without regard to inlet total-pressure recovery and/or increased inlet drag. The air-induction system was investigated with the ducts completely separated by a splitter plate and also with the twin ducts acting as a unit. The following results were obtained:

1. For single-duct operation, increasing the length of zero diffusion in the initial part of the subsonic diffuser from 1 to 3 hydraulic diameters increased the inlet stable subcritical range approximately from 10 percent of critical mass-flow ratio with the shortest to 15 percent with the longest zero-diffusion section.

2. For combined duct operation, bleeding the boundary layer from the compression ramp increased the range of stable flow regulation from 12 percent of critical mass-flow ratio for the no-bleed inlet to 24 percent with the perforated-ramp inlet. Removal of the boundary layer by a flush slot near the inlet throat resulted in a smaller increase in stable mass-flow range, but increased the critical total-pressure recovery by about $2\frac{1}{2}$ percent.

3. Removal of the inlet side fairings did not change the stable range appreciably but did lower the critical total-pressure recovery and the maximum capture mass-flow ratio.

4. At a Mach number of 2.0, stable inlet operation to mass-flow ratios of 40 percent (assumed engine-idle air-flow requirements) could be obtained by increasing the second-ramp angle to 30° to restrict the inlet flow area.

5. Stable regulation to engine-idle air flows at a Mach number of 2.0 was not possible with a second-ramp angle of 0° (simulated a normal-shock inlet).

Lewis Flight Propulsion Laboratory
National Advisory Committee for Aeronautics
Cleveland, Ohio, January 25, 1955

REFERENCES

1. Ferri, Antonio, and Nucci, Louis M.: The Origin of Aerodynamic Instability of Supersonic Inlets at Subcritical Conditions. NACA RM L50K30, 1951.

2. Nettles, J. C.: The Effect of Initial Rate of Subsonic Diffusion on the Stable Subcritical Mass-Flow Range of a Conical Shock Diffuser. NACA RM E53E26, 1953.

3. Bernstein, Harry, and Haefeli, Rudolph C.: Performance of Isentropic Nose Inlets at Mach Number of 5.6. NACA RM E54B24, 1954.

4. Obery, Leonard J., Englert, Gerald W., and Nussdorfer, Theodore J.: Pressure Recovery, Drag, and Subcritical Stability Characteristics of Conical Supersonic Diffusers with Boundary-Layer Removal. NACA RM E51H29, 1952.

5. Fisher, R. E.: Controlling the Subcritical Stability of Conical Shock Inlets. Presented at Symposium on Aerodynamics of Ramjet Supersonic Inlets (Wright-Patterson Air Force Base, Dayton), Oct. 3-4, Marquardt Aircraft Co., 1950.

6. Obery, Leonard J., and Cubbison, Robert W.: Effectiveness of Boundary-Layer Removal Near Throat of Ramp-Type Side Inlet at Free-Stream Mach Number of 2.0. NACA RM E54I14, 1954.

7. Obery, Leonard J., Stitt, Leonard E., and Wise, George A.: Evaluation at Supersonic Speeds of Twin-Duct Side-Intake Systems with Two-Dimensional Double-Shock Inlets. NACA RM E54C08, 1954.

8. Campbell, Robert C.: Performance of a Supersonic Ramp Inlet with Internal Boundary-Layer Scoop. NACA RM E54I01, 1954.

9. Dryer, Murray, and Beke, Andrew: Performance Characteristics of a Normal-Shock Side Inlet Located Downstream of a Canard Control Surface at Mach Number of 1.5 and 1.8. NACA RM E52F09, 1952.

Figure 1. - Photograph of model.

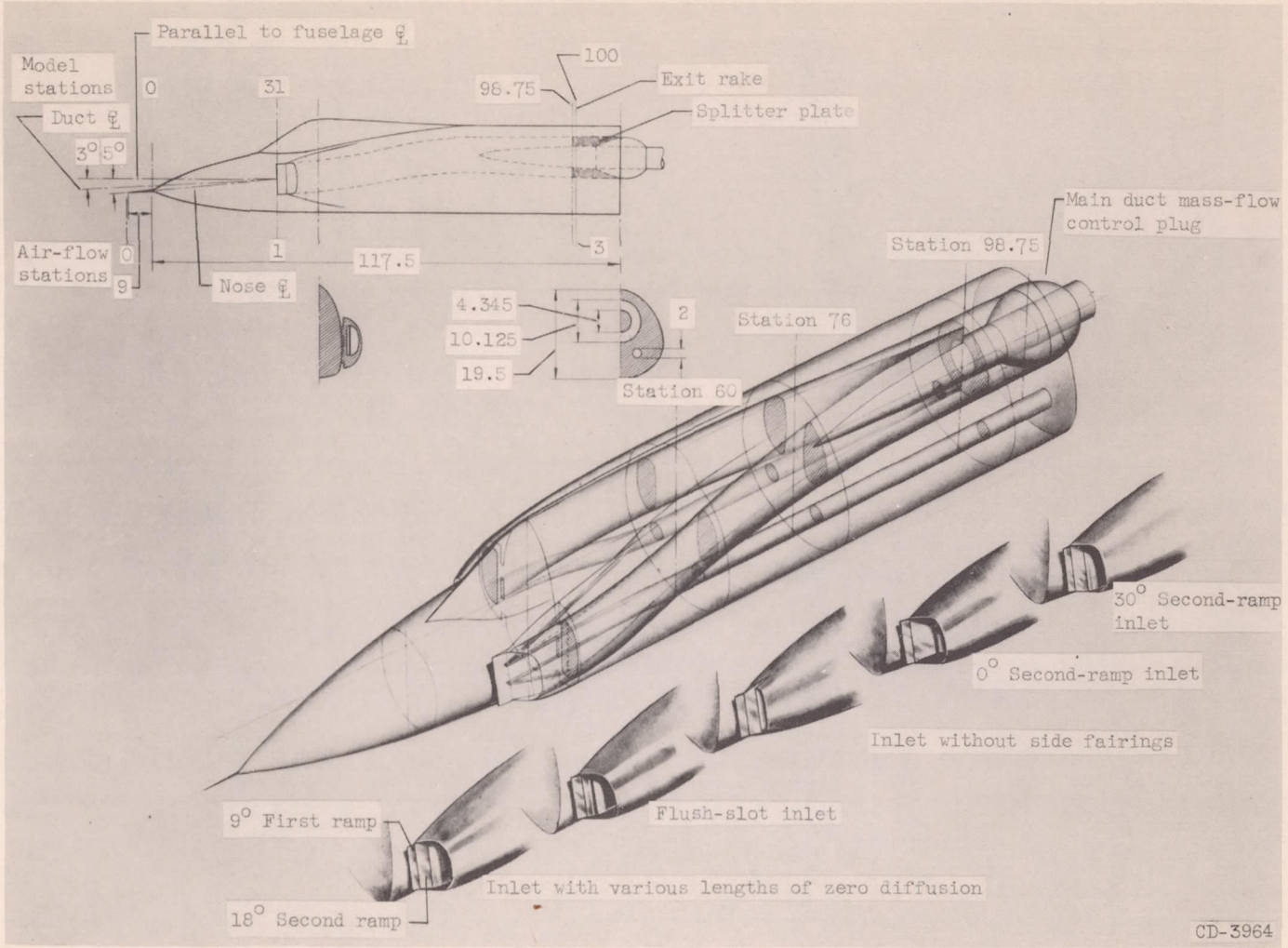

Figure 2. - Diagram of model with representative cross sections. (All dimensions in inches.)

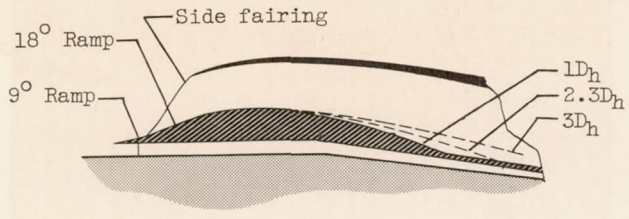

(a) Variations to subsonic diffuser.

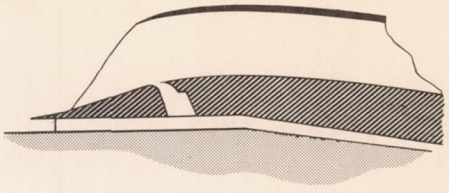

(b) Flush-slot inlet.

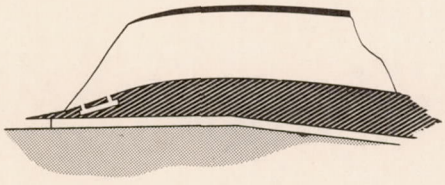

(c) Perforated-ramp inlet.

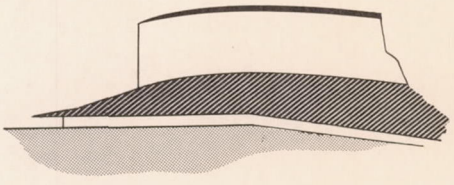

(d) Inlet without side fairings.

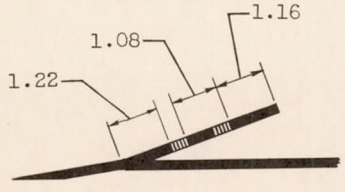

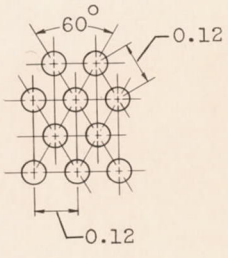

(e) Details of perforated ramp.

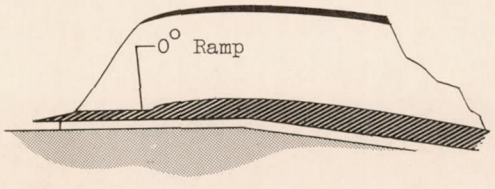

(f) Zero second-ramp inlet.

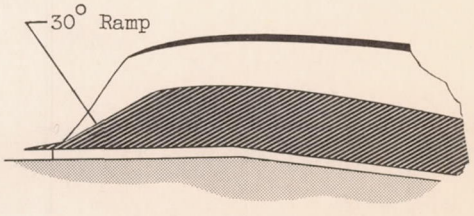

(g) 30° Second-ramp inlet.

CD-3965

Figure 3. - Inlet details. (All dimensions in inches.)

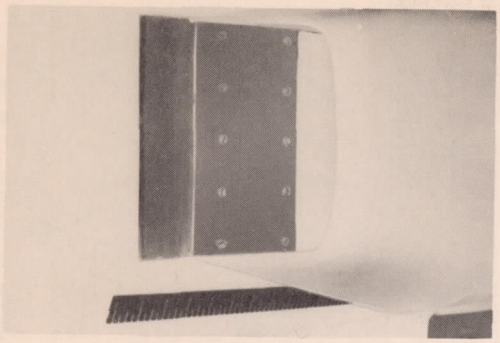

(h) Inlet with various lengths of zero diffusion.

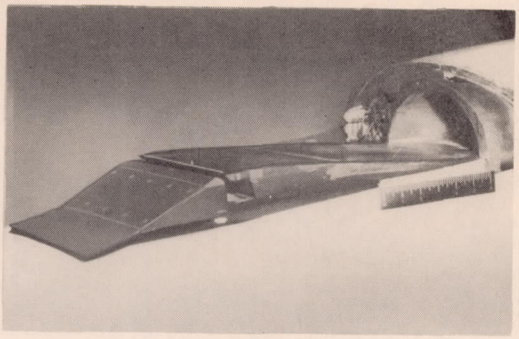

(i) Flush-slot inlet.

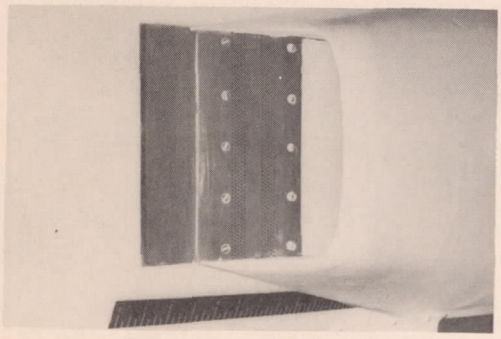

(j) Perforated-ramp inlet.

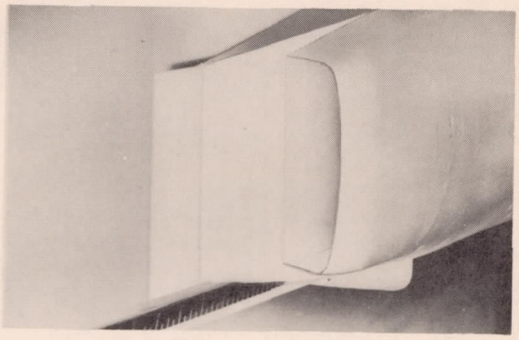

(k) Inlet without side fairings.

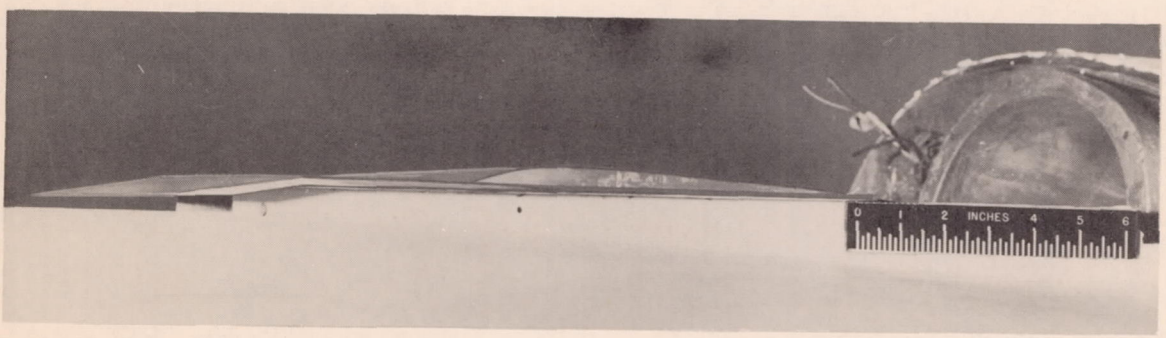

(l) Zero second-ramp inlet.

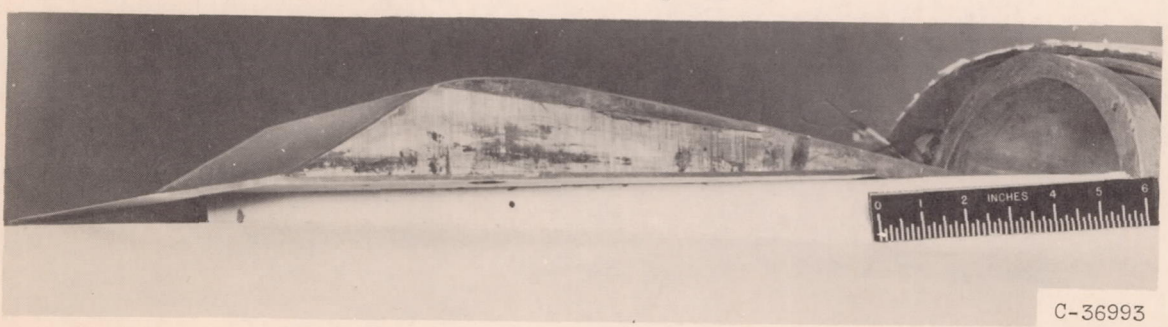

(m) 30° Second-ramp inlet.

Figure 3. - Concluded. Inlet details. (All dimensions in inches.)

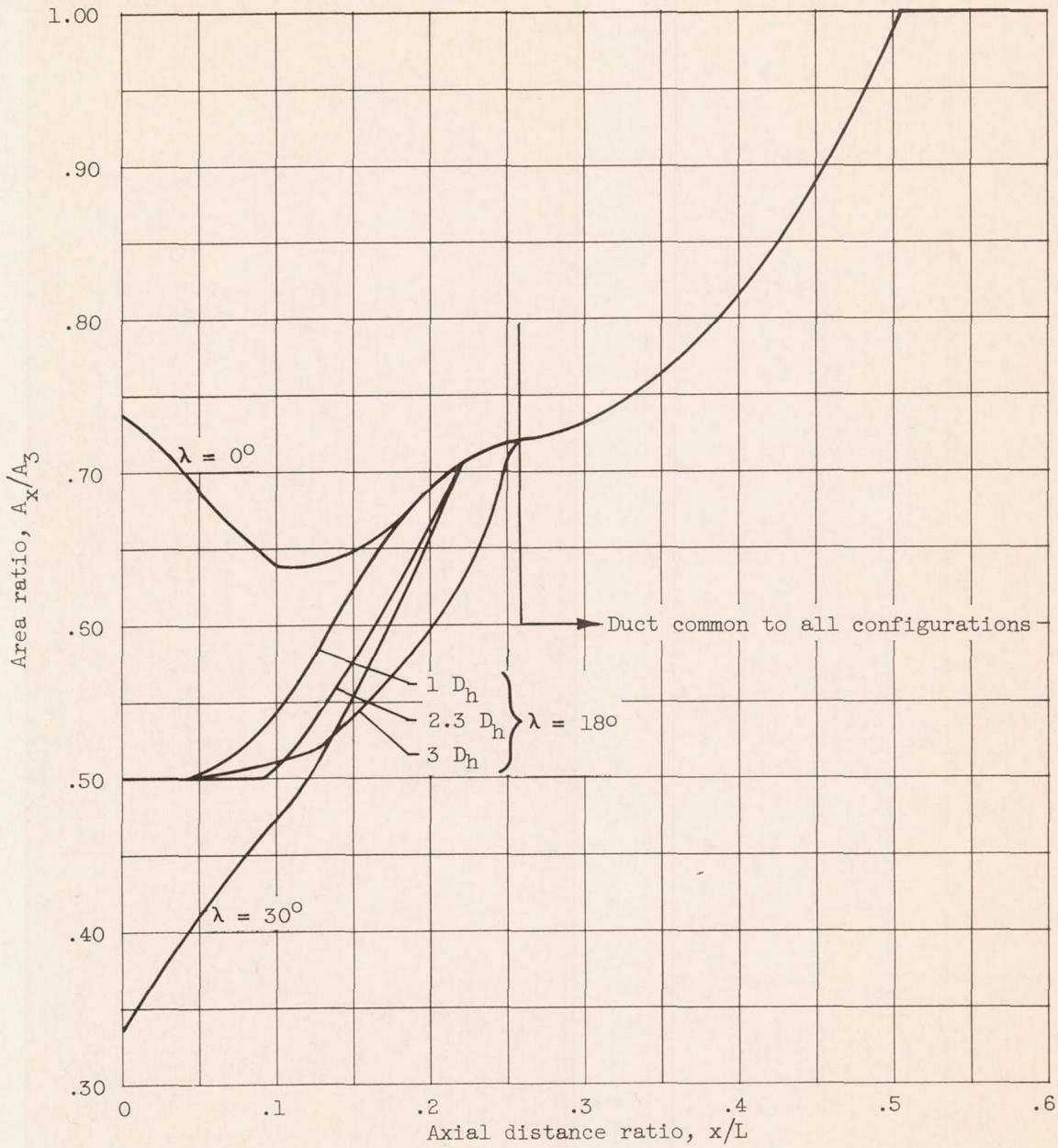

Figure 4. - Area variation of subsonic diffuser; length of subsonic diffuser, 81.5 inches; flow area at diffuser discharge, 0.457 square foot.

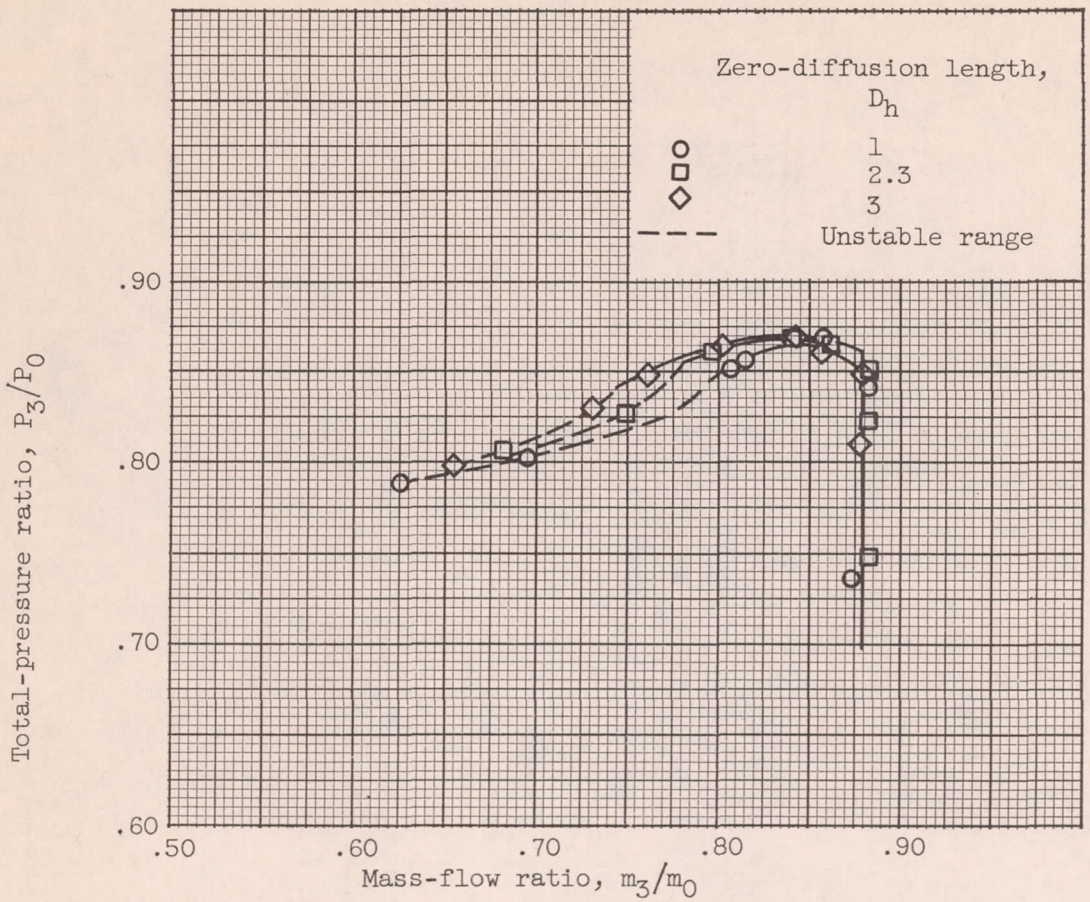

(a) Over-all performance.

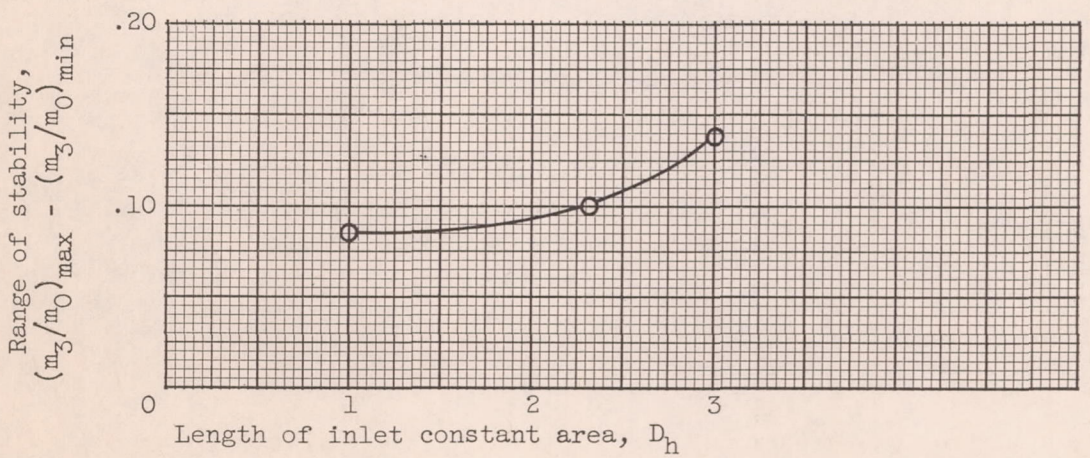

(b) Stability characteristics.

Figure 5. - Effect of inlet constant area sections on performance characteristics of configuration with internal splitter plate; free-stream Mach number, 2.0.

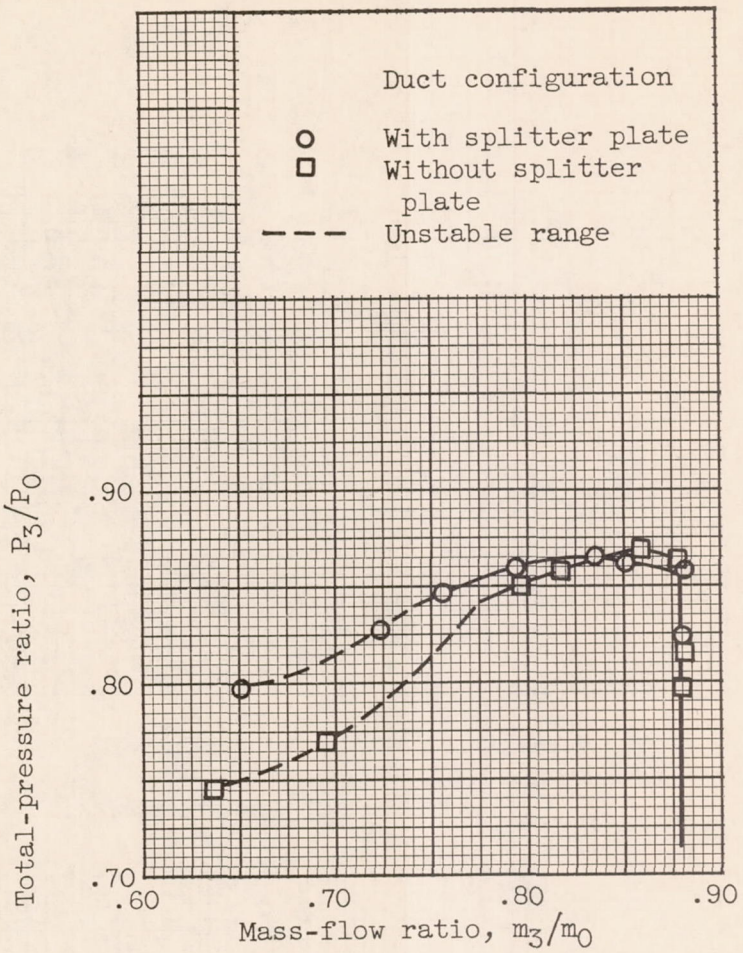

Figure 6. - Effect of splitter plate on inlet performance for configuration with 3-hydraulic-diameter zero-diffusion section; free-stream Mach number, 2.0.

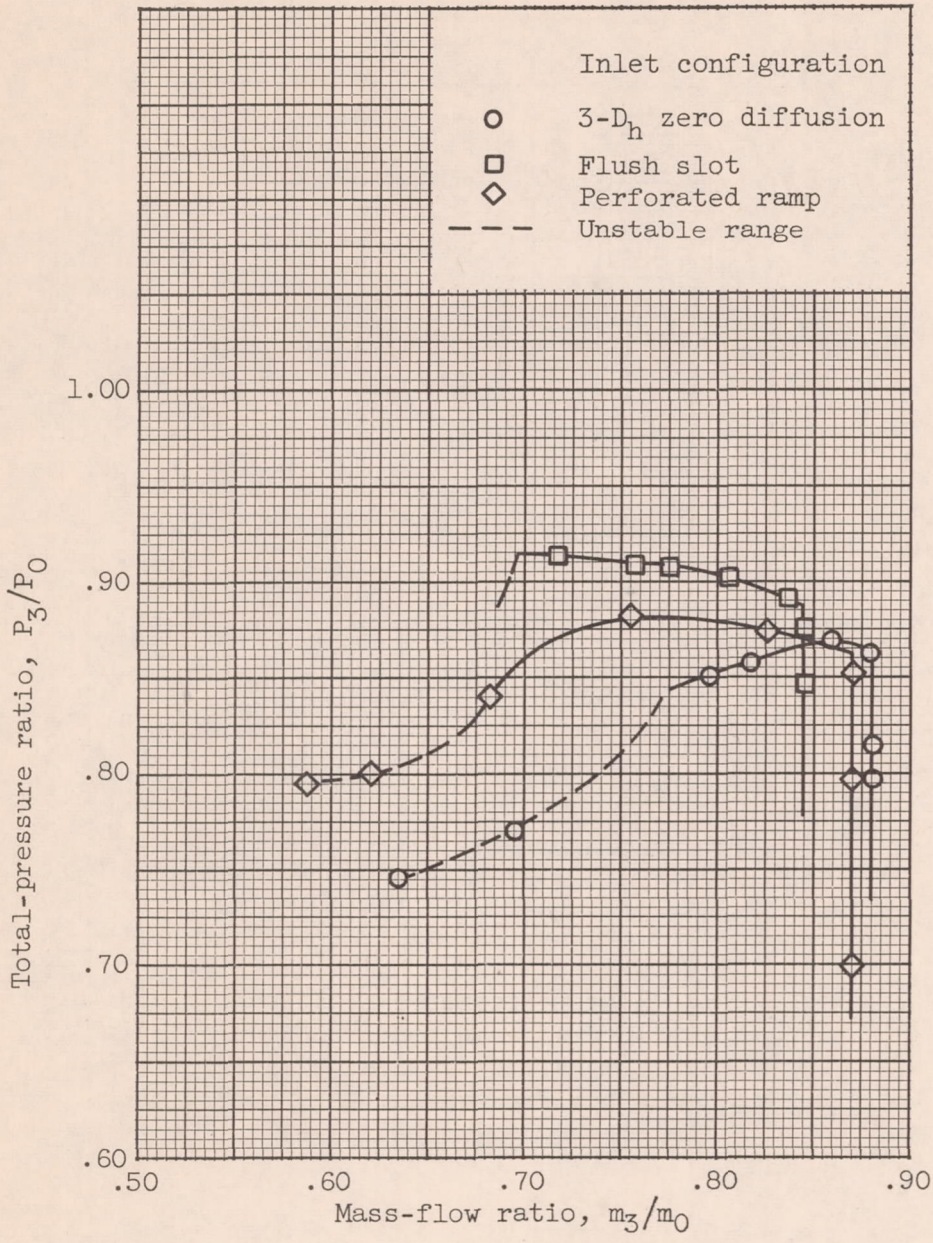

Figure 7. - Effect of boundary-layer control on inlet performance; free-stream Mach number, 2.0.

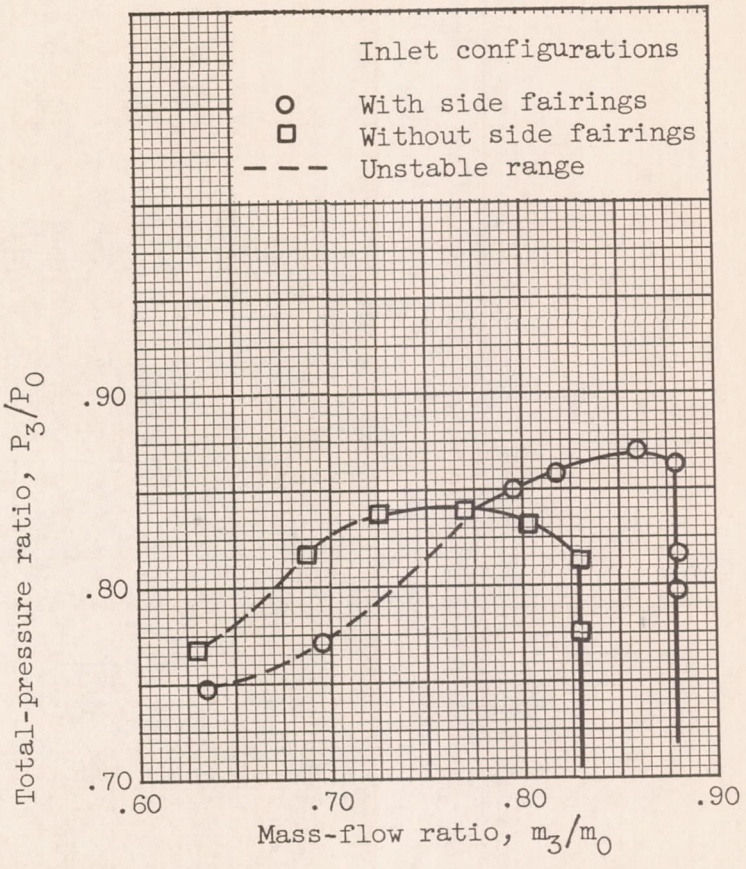

Figure 8. - Effect of side fairing on inlet performance; configuration with 3-hydraulic-diameter zero-diffusion section; free-stream Mach number, 2.0.

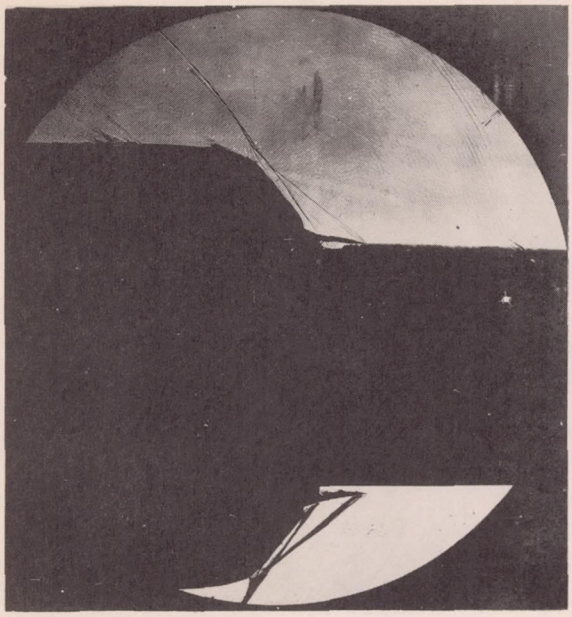

(a) Mass-flow ratio m_3/m_0, 0.88; total-pressure ratio P_3/P_0, 0.76.

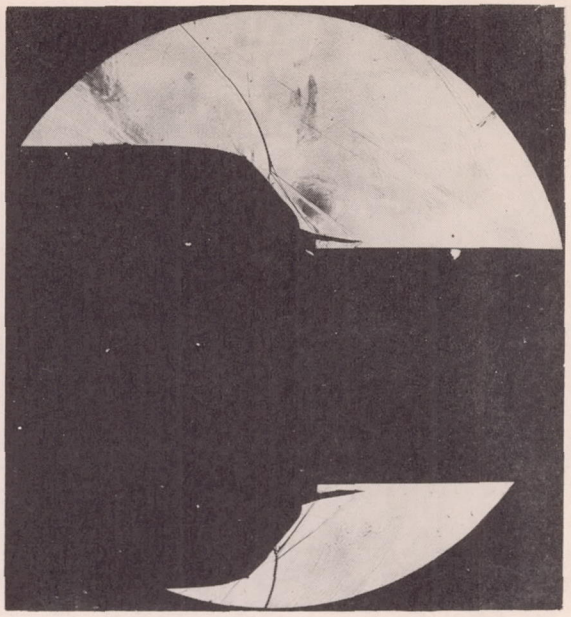

(b) Mass-flow ratio m_3/m_0, 0.832; total-pressure ratio P_3/P_0, 0.838.

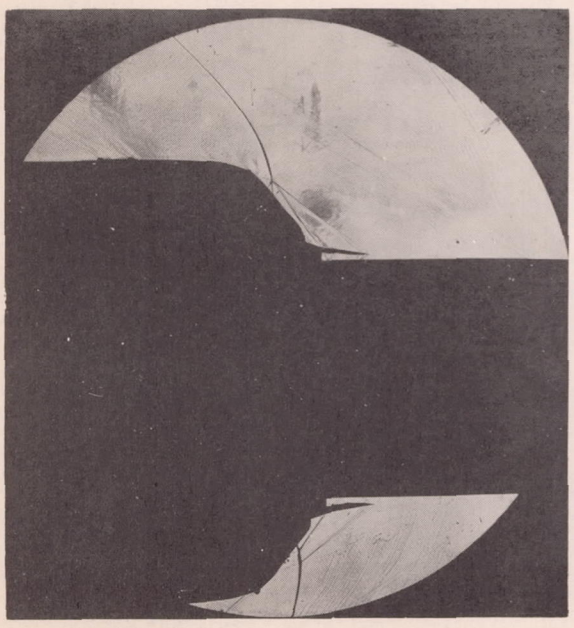

(c) Mass-flow ratio m_3/m_0, 0.695; total-pressure ratio P_3/P_0, 0.845.

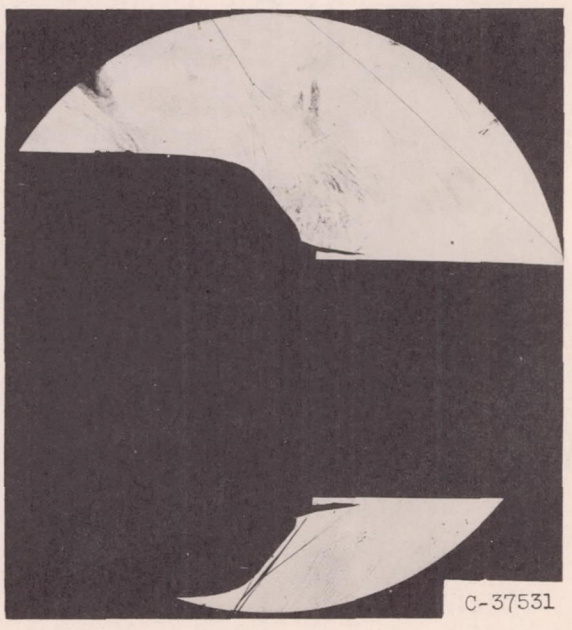

(d) Mass-flow ratio m_3/m_0, 0.373; total-pressure ratio P_3/P_0, 0.571.

Figure 9. - Schlieren photographs of perforated-ramp inlet at Mach number 2.0.

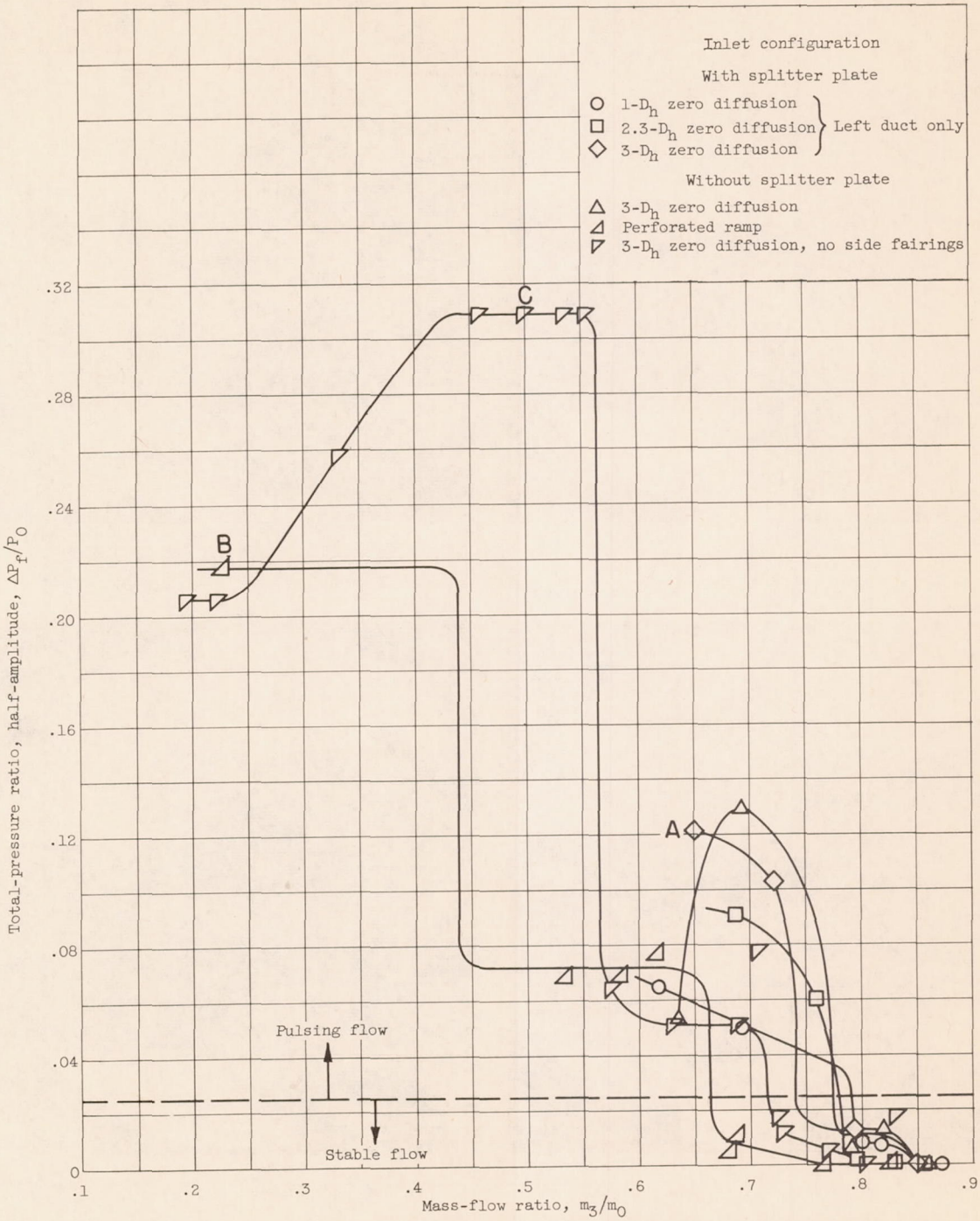

Figure 10. - Maximum total-pressure fluctuation for various inlet configurations; free-stream Mach number, 2.0.

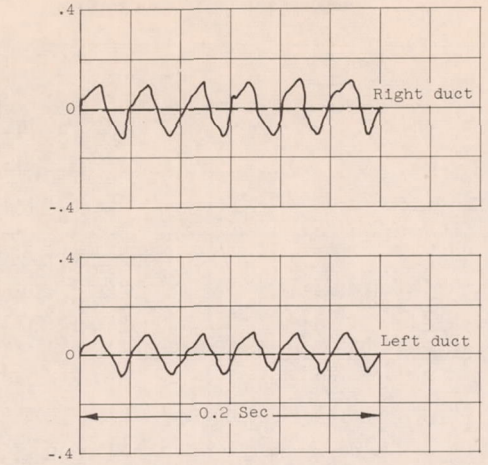

(a) Point A in figure 10; mass-flow ratio m_3/m_0, 0.651; 3-hydraulic-diameter zero diffusion (with splitter plate).

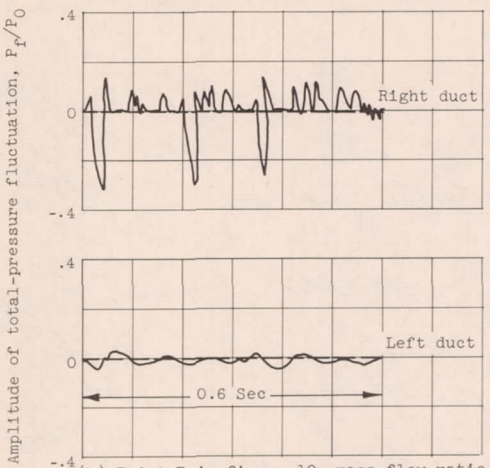

(b) Point B in figure 10; mass-flow ratio m_3/m_0, 0.229; perforated ramp.

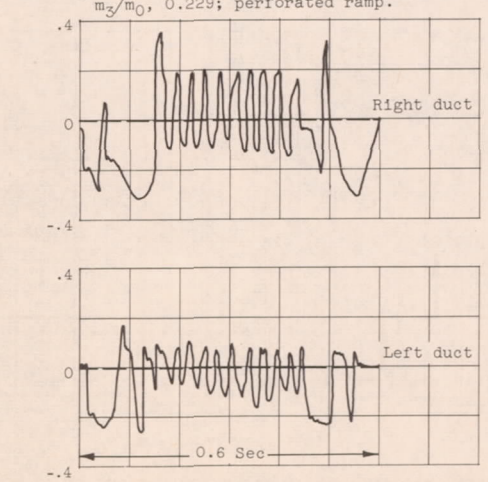

(c) Point C in figure 10; mass-flow ratio m_3/m_0, 0.499; 3-hydraulic-diameter zero diffusion, no side fairings.

Figure 11. - Characteristic wave shapes for various configurations during pulsing.

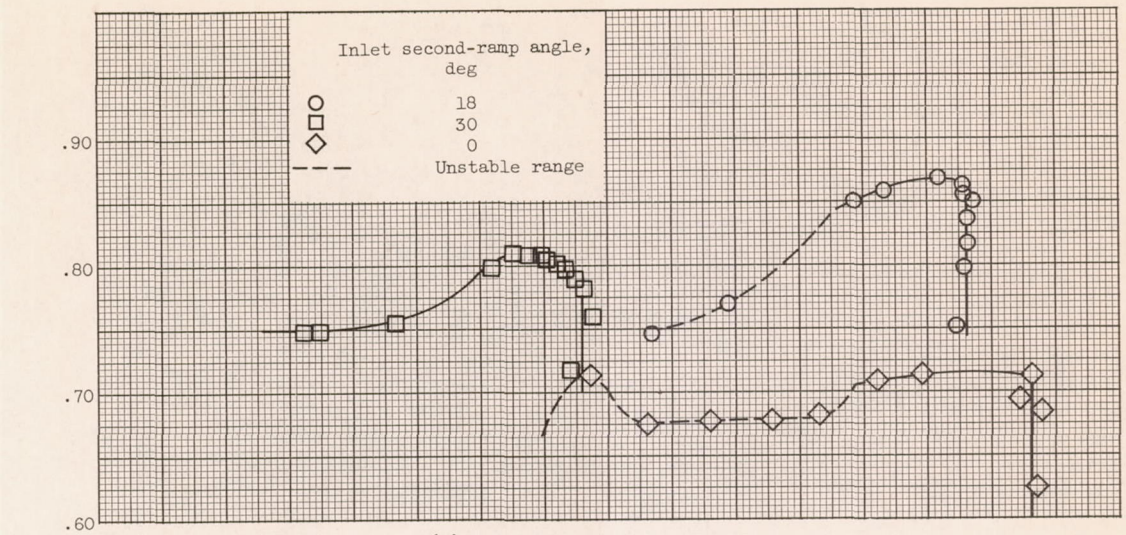

(a) Free-stream Mach number, 2.0.

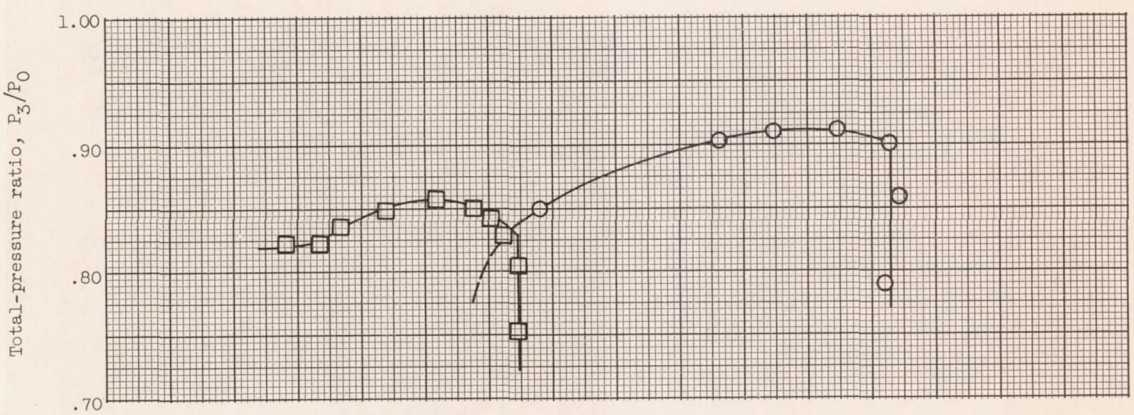

(b) Free-stream Mach number, 1.8.

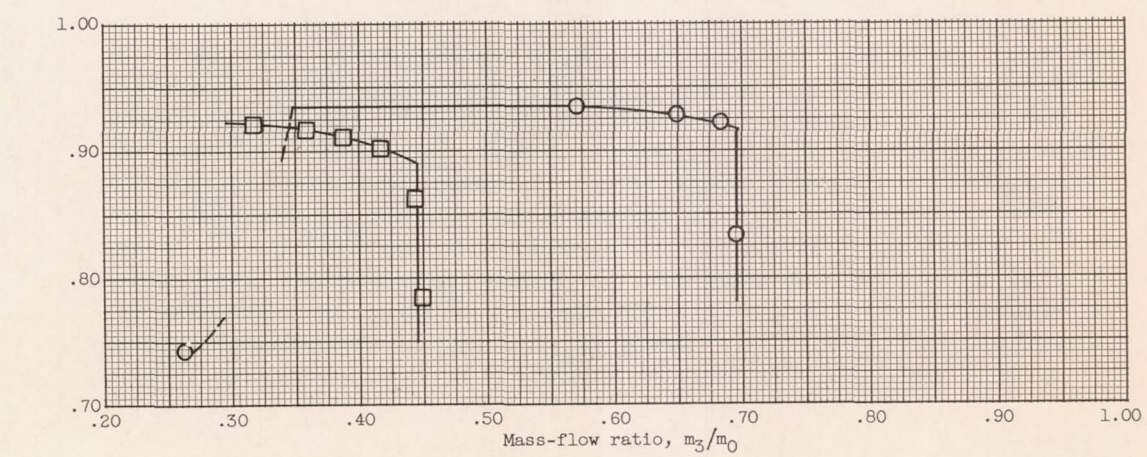

(c) Free-stream Mach number, 1.5.

Figure 12. - Effect of second-ramp angle on inlet performance.

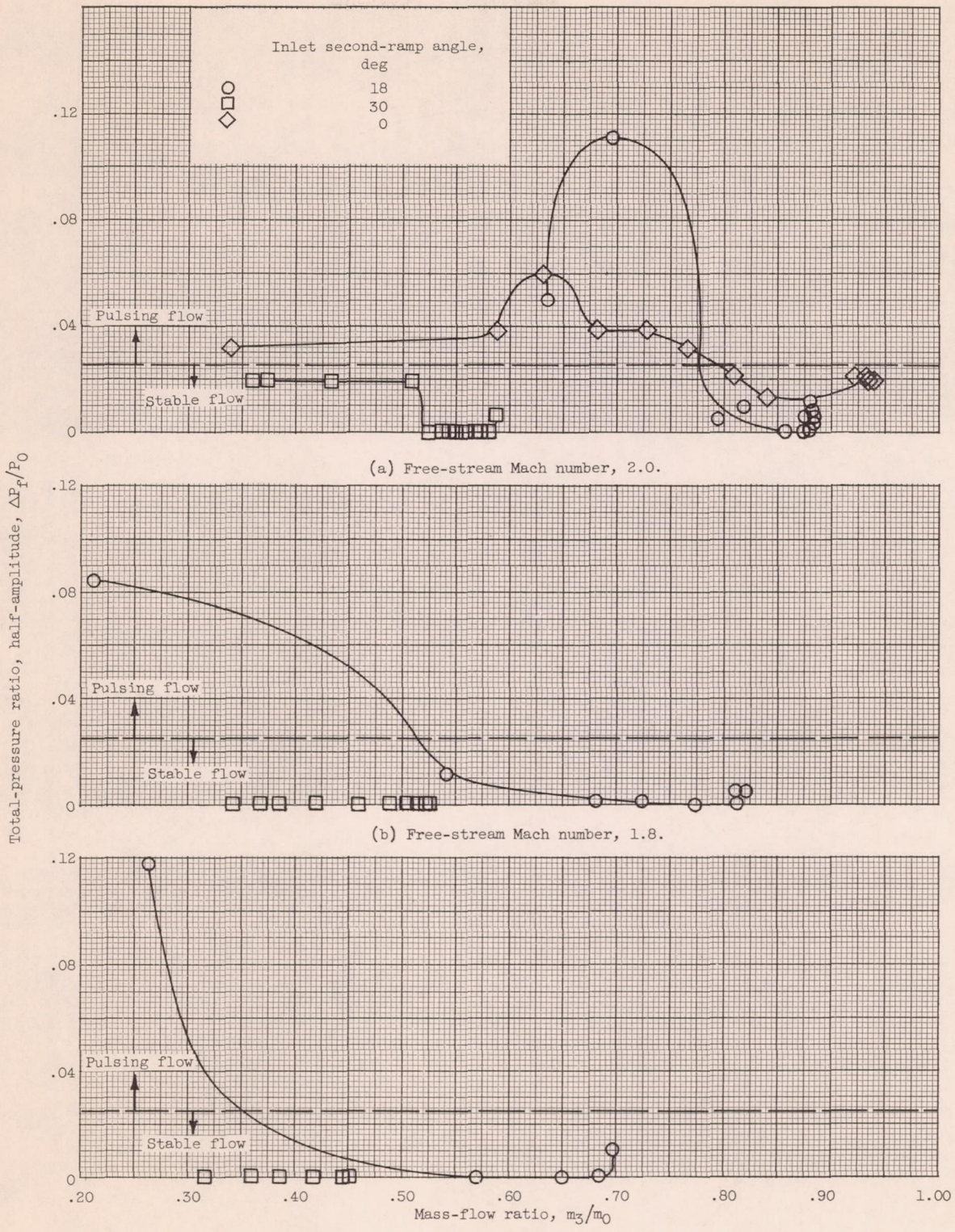

Figure 13. - Maximum total-pressure fluctuation for various inlet configurations.

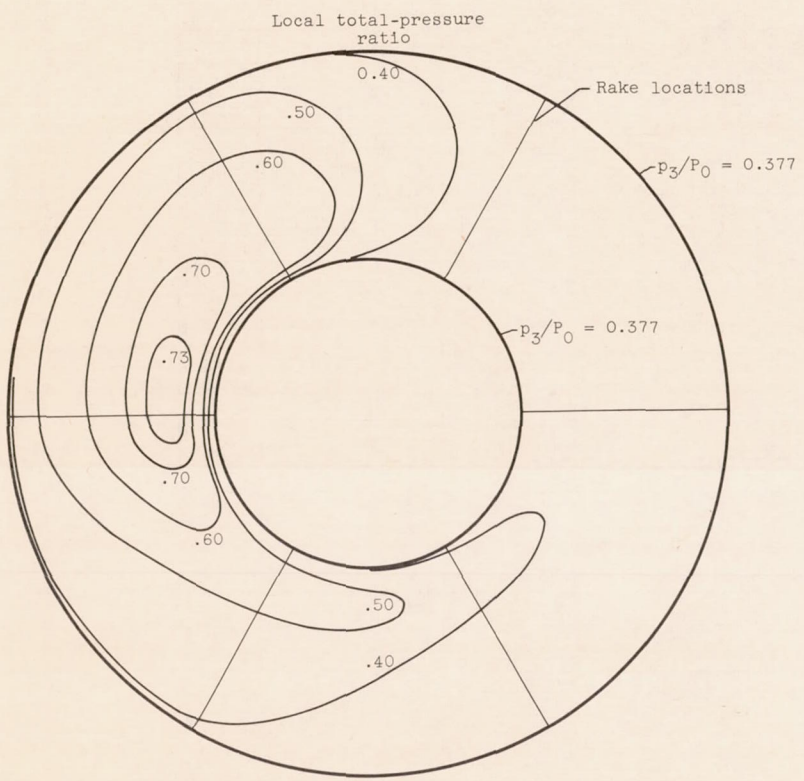

(a) Zero-degree second-ramp inlet; mass-flow ratio m_3/m_0, 0.338; total-pressure ratio P_3/P_0, 0.393.

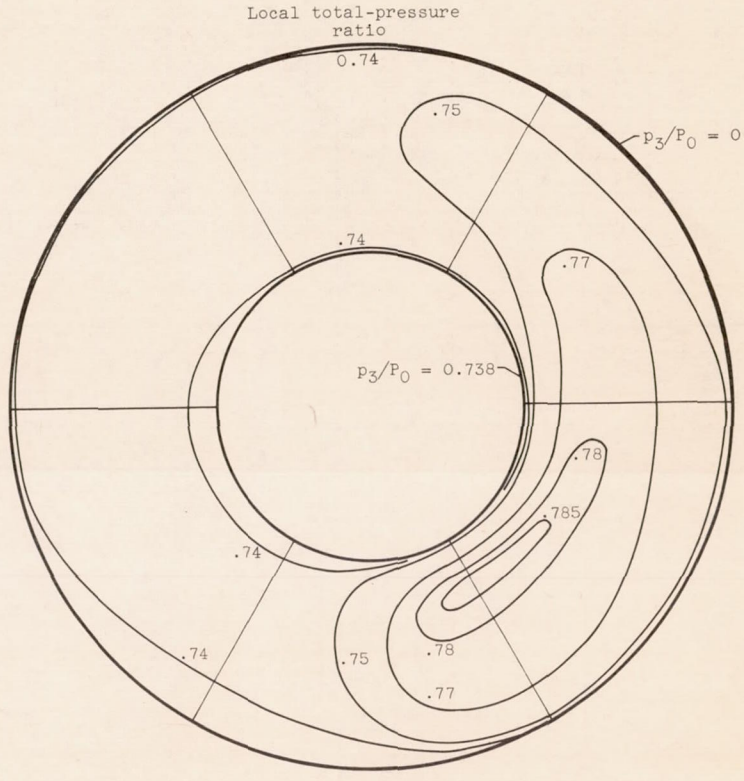

(b) 30° Second-ramp inlet; mass-flow ratio m_3/m_0, 0.362; total-pressure ratio P_3/P_0, 0.747.

Figure 14. - Total-pressure distribution at compressor face; free-stream Mach number, 2.0.

C-37532

(a) Mass-flow ratio m_3/m_0, 0.567; total-pressure ratio P_3/P_0, 0.758.

(b) Mass-flow ratio m_3/m_0, 0.519; total-pressure ratio P_3/P_0, 0.762.

(c) Mass-flow ratio m_3/m_0, 0.357; total-pressure ratio P_3/P_0, 0.748.

Figure 15. - Schieren photographs of 30° second-ramp inlet at Mach number 2.0.